scientific reports

Check for updates

OPEN

Damage constitutive model and experimental study of deep coal rock under thermal-hydro-mechanical coupling

Kunhong Lv[1], Hui Zhang[1]✉, Baokang Wu[1], Boyuan Yang[1], Yuting Zhou[1], Xingyu Li[1], Xu Luo[2,3] & Jintao An[1,4]

This study investigates the thermal-hydro-mechanical (THM) coupled damage behavior of deep coal rocks from the Benxi Formation in the Ordos Basin. By conceptualizing coal rock as a dual-porosity medium comprising fractures and matrix, a damage constitutive model was developed through the integration of the Lemaitre strain equivalence hypothesis, continuum damage mechanics, and thermodynamic principles. The model introduces damage variables and correction coefficients to characterize the synergistic effects of confining pressure, temperature, and drilling fluid infiltration. Experimental validation was performed using a custom-designed multi-field coupled triaxial testing system, with triaxial compression tests conducted across varying confining pressures, temperatures, and moisture content conditions. The results show that: (1)The proposed constitutive model successfully quantifies damage evolution under HTM coupling, where parameter *q* governs residual deformation characteristics and parameter *n* modulates post-peak stress degradation trends; (2) Drilling fluid immersion induces time-dependent mechanical deterioration, significantly reducing peak stress and elastic modulus, with increasing moisture content exacerbating nonlinear degradation effects; (3)Macroscopic failure modes transition from tensile-shear conjugate patterns to single shear planes as confining pressure decreases and moisture content increases; (4)Theoretical stress-strain curves demonstrate strong consistency with experimental data, validating the model's capability to simulate deformation laws and damage accumulation processes. The research establishes a theoretical framework for analyzing wellbore instability mechanisms in deep coalbed methane reservoirs, providing critical insights for drilling fluid optimization and geomechanically risk mitigation strategies.

Keywords Coal, Damage variables, Constitutive model, Mechanical properties, Thermal-hydro-mechanical coupling

The exploration and development targets for coalbed methane in China are mainly shallow (depth < 1000 m) and deep (depth < 2000 m). With the increase in energy demand and development level, the number of coal seam methane blocks that can be efficiently exploited on a large scale is gradually decreasing. The exploration and development goals also include expanding from shallow coal seam methane to medium shallow coal seam methane and deep (burial depth > 2000 m) coal rock methane[1,2]. With the substantial investment of China's major oil and gas companies, deep coal rock gas has become the main battlefield of China's fossil energy exploration and development. The main exploration and development areas are mainly distributed in the Ordos Basin, the Junggar Basin, and the Qinshui Basin[3,4]. Damage is an effective measure of the degree of rock deformation and failure. In recent years, scholars at home and abroad have made significant achievements in studying coal rock damage theory.

In terms of coal rock damage experiments, Yin et al.[5] conducted deformation characteristics and compressive strength tests on gas-containing coal samples under varying confining pressures and gas pressures. Yu et al.[6] investigated the acoustic emission and damage evolution characteristics of coal rocks under different confining

[1]School of Petroleum Engineering, China University of Petroleum (Beijing), Beijing 102249, China. [2]School of Materials and Chemistry, Southwest University of Science and Technology, Mianyang 621010, China. [3]Jiangsu Key Laboratory for Construction Materials, Southeast University, Nanjing 211189, China. [4]College of Petroleum Engineering, China University of Petroleum (Beijing) at Karamay, Karamay 834000, China. ✉email: zhanghui168_vip@163.com

pressures. Lai et al.[7] studied the softening effects and multi-scale damage evolution of coal under hydraulic coupling. Similarly, Yu et al.[8] explored the impact of drilling fluid on the compressive strength, elastic modulus, and deformation characteristics of coal rocks. Li et al.[9–11] focused on the evolution of coal rock damage and mechanical properties under varying water contents, confining pressures, gas pressures, and temperatures. Gao et al.[12] conducted experiments to assess the effects of temperature, confining pressure, and gas pressure on coal rock mechanics. Yu et al.[13] performed X-Ray Diffraction (XRD) analysis on coal samples saturated at varying water pressures. They also utilized Scanning Electron Microscopy (SEM), Nuclear Magnetic Resonance (NMR), Acoustic Emission (AE), and conventional triaxial tests to explore the internal water migration patterns and mechanical damage characteristics of coal samples under different water contents. Fu and Han et al.[14,15] studied the internal mechanisms of coal rock damage under various pressure and immersion conditions. These investigations provide valuable insights into the factors influencing the damage process of coal rock. However, existing research results mainly focus on shallow coal rocks, lacking research on the mechanical properties and damage mechanisms of deep coal rocks with a burial depth greater than 2000 m. When characterizing the damage and failure process of deep coal rocks, it is necessary to consider the combined effects of temperature, stress, and drilling fluid immersion on the degradation of coal rock damage.

In terms of constitutive models for coal rock damage, Dai et al.[16] obtained damage constitutive models and damage evolution equations for coal rock at different damage stages. Yi et al.[17–19] introduced endochronic theory and anisotropic damage factors in their damage constitutive models for gas-containing coal rock. Zhang et al.[20] proposed a coupled damage-fluid mechanics model that accounts for stress, damage, and permeability in coal deformation. In addition, other models, such as those by Hu et al.[21] and Li et al.[10]consider the effects of gas expansion, moisture content, and hydro-mechanical coupling on coal rock's damage evolution. Zhu et al.[22] developed a segmented damage-permeability model for coal rock. Similarly, Ding et al.[23] formulated a damage evolution equation and a mechanical constitutive model for gas-bearing coal rock, incorporating factors such as initial porosity, matrix expansion due to adsorbed gas, the softening effect of gas migration, and the true triaxial stress state. Fan et al.[24] proposed a nonlinear (non-Darcy) thermal-hydro-mechanical damage model based on equivalent matrix scale and dynamic diffusion (EDN-THMD). Deng et al.[25] introduced a temperature-stress-time coupled damage variable, employing a time-varying negative exponential function. Du et al.[26] developed a dynamic damage equation for raw coal samples under uniaxial compression, establishing a quantitative relationship between the damage variable and volumetric strain energy under true triaxial stress conditions. Fu et al.[14] derived a statistical damage constitutive model characterizing the overall stress-strain relationship of coal rock. Han et al.[15] proposed a damage constitutive model describing the entire deformation process of coal samples under long-term water immersion. Ye et al.[27] derived a three-coupling damage variable considering pore, crack, and thermal damage and established a damage-permeability model for dual-porosity coal under thermal-mechanical coupling. Shen et al.[28] derived a dissipative energy evolution equation based on a logistic function, developing a three-dimensional damage constitutive model for coal that incorporates residual strength. These contributions highlight the need for comprehensive models that consider multiple factors affecting coal rock behavior under complex conditions. However, existing modeling methods mainly focus on single temperature effects or stress damage, often neglecting the impact of drilling fluid immersion on coal rocks. In addition, the damage mechanism under the coupling effect of the three factors has not been fully studied and needs further exploration.

This paper takes deep coal rocks in the Ordos Basin as the research object. Firstly, assuming that deep coal rocks are a dual medium combination of fractures and matrix, based on the Lemaitre strain equivalence hypothesis, continuous damage mechanics, and thermodynamics, the damage variables of coal rocks under the coupling of thermal-hydro-mechanical are derived, and a deep coal rock damage constitutive model is finally established. Then, with the help of a self-developed multi-field coupling triaxial testing system, triaxial compression tests were conducted under different confining pressures, temperatures, and moisture contents, and the stress-strain characteristics, mechanical characteristics, and failure characteristics of deep coal rocks were obtained. Finally, relying on the experimental results, the rationality and reliability of the model were verified, and a sensitivity analysis of model parameters and a study on damage evolution laws was conducted. The research results deepen the understanding of the mechanical behavior characteristics of deep coal rocks, providing theoretical support and experimental reference for the prevention of wall instability in deep coal gas horizontal wells.

Damage constitutive model

Damage variable of coal rock drilling fluid effect

In the environment of drilling fluid immersion, under the continuous action of degradation mechanisms such as hydration reaction, weak surface structures such as micro-cracks in coal rock continue to expand and propagate, mechanical properties deteriorate, and damage accumulates gradually. The water-soaked weakening process of coal rock usually includes two states: unsaturated weakening and saturated weakening, and its water content determines the mechanical properties. Assuming that the damage of coal rock with a water content of 0% is 0, according to the elastic modulus method proposed in continuum mechanics, the damage variable of coal rock under different water contents can be defined as[10,15]

$$D_W = 1 - \frac{E_W}{E_0} \tag{1}$$

Where D_W is the damage variable with a moisture content of W; E_0 is the elastic modulus of coal rock with a moisture content of 0%; E_W is the elastic modulus with a moisture content of W.

The following formula can express the elastic modulus at different moisture contents

$$E_{\mathrm{w}} = iE_{\mathrm{ws}} + jE_{\mathrm{wt}}, \begin{cases} i = 1, j = 0, & \text{if unsaturation} \\ i = 0, j = 1, & \text{if saturation} \end{cases} \tag{2}$$

Where E_{ws} is the elastic modulus of the coal sample at saturation S; E_{wt} is the elastic modulus of the saturated coal sample with a soaking time of t; i and j are saturation parameters; When the coal sample is in the unsaturated state, the value of j is 0, and the value of i is 1; When the coal sample is in saturation state, the value of j is 1, and the value of i is 0.

Damage variable of coal rock under temperature effect

Under the action of temperature, thermal stress is generated inside the coal rock, causing the expansion and mutual extrusion of coal rock mineral particles and the continuous expansion and connection of micro-cracks such as cleats, destroying mechanical properties. Assuming that the rock does not undergo thermal damage at 25 °C, and based on macroscopic damage mechanics theory, the rock damage variable under temperature action (D_T) can be defined by introducing the macroscopic mechanical parameter elastic modulus[29]which is

$$D_T = 1 - \frac{E_T}{E_{25}} \tag{3}$$

Where E_T is the elastic modulus at temperature T; E_{25} is the elastic modulus at 25℃.

Damage variable of coal rock under load

The Lemaitre strain equivalence hypothesis states that the effective stress acting on a damaged material can be represented by the nominal stress acting on a non-damaged material, and the constitutive relationship of damaged coal rock can be expressed as follows[9]

$$[\sigma^*] = [\sigma]/(1 - D_M) = [C][\varepsilon]/(1 - D_M) \tag{4}$$

Where $[\sigma^*]$ is the effective stress tensor; $[\sigma]$ is the nominal stress tensor; $[\varepsilon]$ is the strain tensor; $[C]$ is the elastic modulus tensor; D_M is the damage variable of rock.

Considering the residual strength after the failure of coal rock, a damage correction factor (q) is introduced to correct the effective stress of coal rock[10,30]

$$[\sigma^*] = [\sigma]/(1 - qD_M) = [C][\varepsilon]/(1 - qD_M) \tag{5}$$

The coal rock structure is heterogeneous, with a large number of primary pores and fractures randomly distributed within it, and these pores and fractures continue to sprout, extend, and accumulate as the load is applied. The mechanical properties of coal rock vary depending on the distribution characteristics of pores and fractures. Dividing coal rock into sufficiently small microelements, as the rock's stress state changes, the microelements' destruction is random[31,32]. The brittle characteristics of coal rock are relatively obvious, and the deformation of coal rock under external load conditions in the pre-peak stage is considered to be elastic deformation with unclear plastic deformation characteristics. Therefore, the traditional Weibull probability distribution model cannot accurately describe coal rock's damage and failure characteristics[10]. Based on the principles of elastic damage mechanics, this paper assumes that the initial strain of coal rock changes linearly and describes the damage variables of microelements under load in segments

$$D_M = \begin{cases} 0 & \varepsilon_1 < \varepsilon_p \\ 1 - (\varepsilon_p/\varepsilon_1)^n & \varepsilon_p \le \varepsilon_1 \le \varepsilon_{\mathrm{cr}} \\ 1 - \lambda\varepsilon_p/\varepsilon_1 & \varepsilon_1 \ge \varepsilon_{\mathrm{cr}} \end{cases} \tag{6}$$

Where ε_p is the strain at peak stress; ε_{cr} is the compressive strain at residual compressive strength; ε_1 is the axial strain; λ is the residual strength coefficient; n is the damage constitutive coefficient.

Total damage variable of coal rock under hydro-mechanical-thermal coupling effect

Assuming that the damage caused by temperature and drilling fluid to coal rock has been completed before the load is applied, the sum of the damage caused by temperature and drilling fluid to coal rock is defined as external damage (D_N), expressed as

$$D_N = D_T + D_W \tag{7}$$

Based on the external damage of coal rock, further loading causes load damage to coal rock. There is a certain coupling relationship between load damage and external damage, and the total damage of coal rock is not simply a simple superposition of the two. Considering the residual strain damage correction factor, the total damage of coal rock (D) should be expressed as

$$D = D_N + qD_M - qD_M D_N \tag{8}$$

Constitutive equation of coal-rock damage under hydro-mechanical-thermal coupling

Assuming that coal rock is an isotropic material, and the elastic phase of the stress-strain relationship of coal rock conforms to the generalized Hooke's law, according to the Lemaitre strain equivalence hypothesis[30]the constitutive relationship of coal damage can be expressed as:

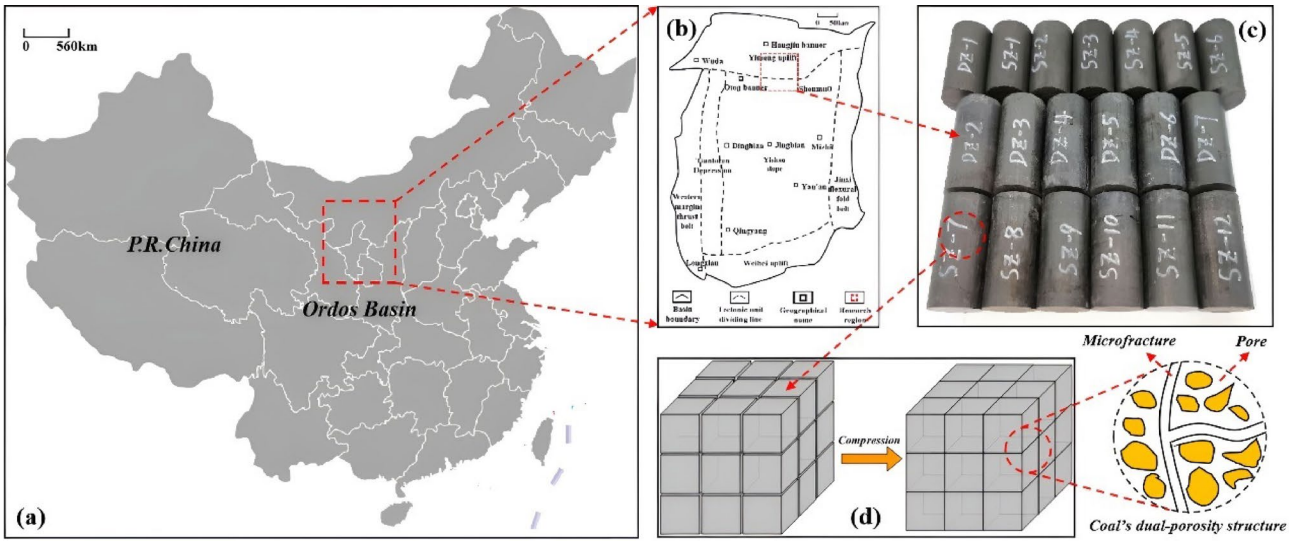

Fig. 1. Specimen position and structure; (**a**) locations of the Ordos basin; (**b**) locations of the gas field from which the coal samples were obtained; (**c**) photos of coal samples; (**d**) coal's dual-porosity structure.

Sample	Industrial analysis/%				Element analysis/%				
	M_{ad}	A_{ad}	V_{ad}	FC_{ad}	S	O	C	H	N
Coal sample	1.68	7.62	14.15	76.55	0.28	7.63	83.14	4.58	4.34

Table 1. Experimental results of the basic physical characteristics in coals (M: moisture content; A: Ash content; V: volatile matter; FC: fixed carbon; ad: air drying basis; S: sulfur; O: oxygen; C: carbon; H: hydrogen; N: Nitrogen).

$$\sigma_1 = E\varepsilon_1 (1 - qD_M) + 2u\sigma_3 \tag{9}$$

Where σ_1 and σ_3 are axial pressure and confining pressure, respectively; E is the elastic modulus; μ is the Poisson's ratio of coal rock.

Considering the effects of drilling fluid immersion and temperature on coal rock damage, the elastic modulus of coal rock after combined degradation is defined as , and its expression is

$$E = (1 - D_N)E_0 \tag{10}$$

By combining Eqs. (1), (2), and (10), we obtain

$$E = E_0 (1 - D_w)(1 - D_T) \tag{11}$$

Under the combined action of thermal-hydro-mechanical coupling, coal rock exhibits different damage characteristics. Substituting Eq. (11) into Eq. (9) yields

$$\sigma_1 = E_0\varepsilon_1 (1 - D_w)(1 - D_T)(1 - qD_M) + 2u\sigma_3 \tag{12}$$

By combining Eqs. (7), (8), and (12), we can derive the constitutive model for segmented damage of coal rock under the coupling of thermal-hydro-mechanical

$$\sigma_1 = \begin{cases} E_0\varepsilon_1 (1 - D_w)(1 - D_T)(1 - qD_M) + 2u\sigma_3 & \varepsilon_1 < \varepsilon_{co} \\ E_0\varepsilon_1 (1 - D_w)(1 - D_T)[1 - q + q(\varepsilon_p/\varepsilon_1)^n] + 2u\sigma_3 & \varepsilon_{c0} \le \varepsilon_1 \le \varepsilon_{cr} \\ E_0\varepsilon_1 (1 - D_w)(1 - D_T)(1 - q - q\lambda\varepsilon_p/\varepsilon) + 2u\sigma_3 & \varepsilon_1 \ge \varepsilon_{cr} \end{cases} \tag{13}$$

Experimental work

Selection and preparation of coal samples

The coal samples used in the experiment were taken from the Benxi Formation in the Ordos Basin, as shown in Fig. 1. Table 1 shows the industrial and elemental analysis results of the coal seams to which the experimental coal samples belong. The industrial analysis shows that the moisture content of the coal sample is 1.68%, the ash content is 7.62%, the volatile content is 14.15%, and the fixed carbon is 76.55%. It has the characteristics of low moisture, ultra-low ash, and low volatility. The industrial analysis shows that the coal sample contains 0.28%

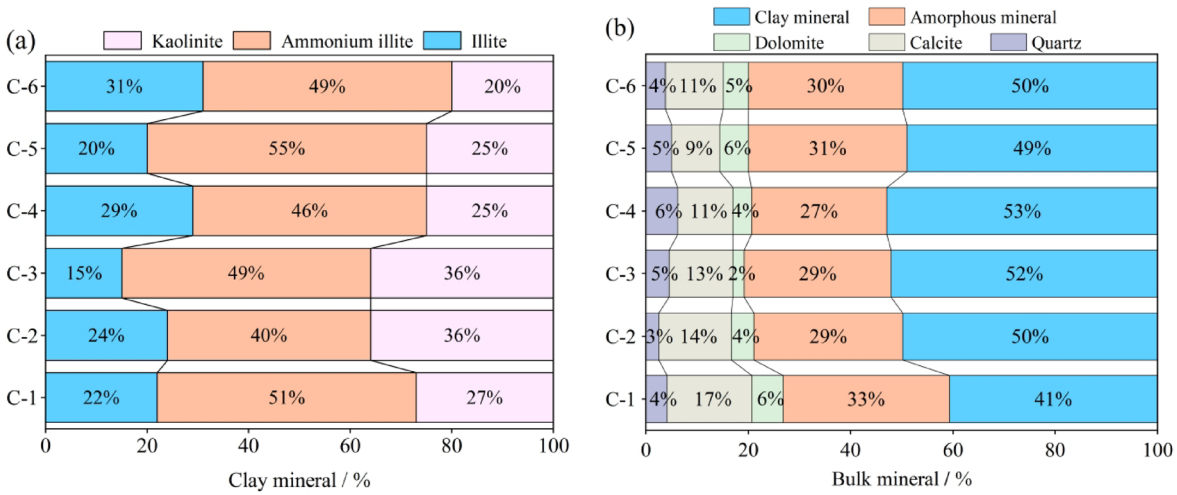

Fig. 2. Test results of mineral components.

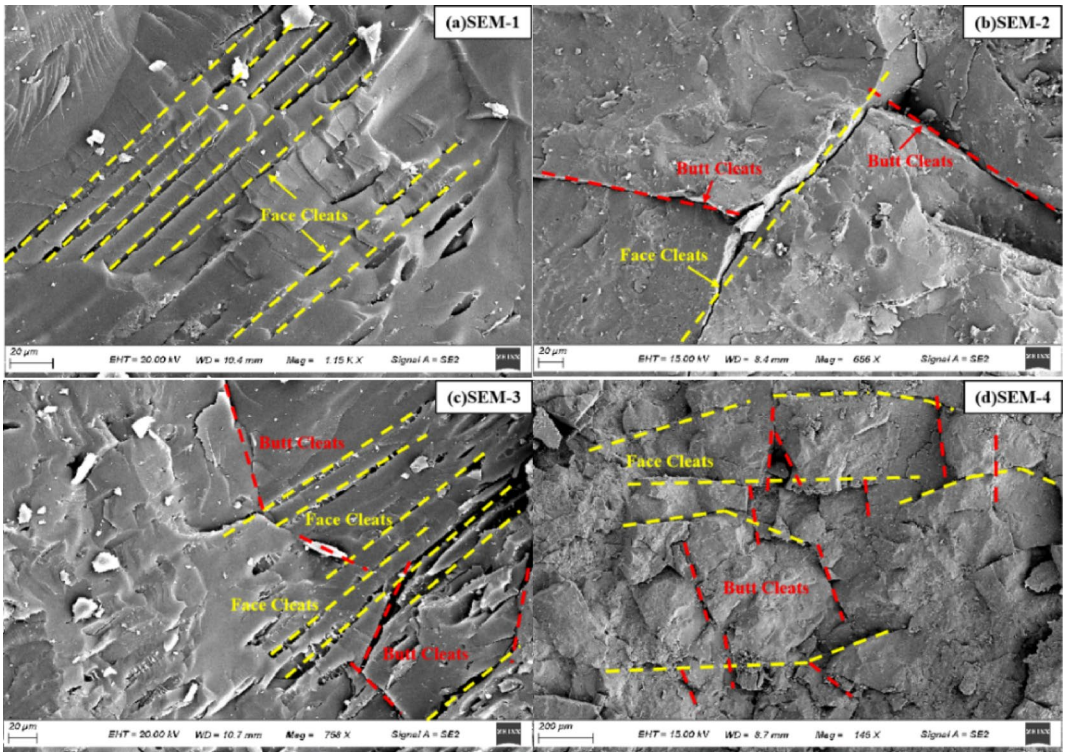

Fig. 3. Schematic diagram of scanning electron microscope.

sulfur, 7.63% oxygen, 83.14% carbon, 4.58% hydrogen, and 4.34% nitrogen, which has the characteristics of ultra-low sulfur. Figure 2 shows the XRD mineral composition test results of coal samples. It can be seen that the main whole rock mineral components and their mass fractions of coal samples are clay minerals (41%~53%), amorphous minerals (27%~33%), dolomite (2%~6%), calcite (9%~17%), and quartz (3%~6%); the clay mineral components and mass fractions are kaolinite (20–36%), ammonium illite (40%~55%), and illite (15%~31%). Figure 3 shows the coal sample's SEM micrograph. It can be seen that the coal sample has developed cracks and pores, with faceted and end cleats interlaced and cut in a dendritic and reticulated structure, providing channels for drilling fluid leakage and easily causing wellbore instability.

It can be seen that the coal sample surface is dense, with internal cracks and pores developed, and the surface and end cleats are interlaced and cut, distributed in a dendritic and reticulated structure. Due to the particularity of its structure and properties, it is difficult to coring coal rock. Therefore, the coring position should be arranged reasonably to avoid primary weak surfaces such as bedding and natural fractures. The original coal sample

obtained from coring is drilled along the vertical bedding plane direction using a coring machine. Then multiple standard cylindrical samples with a size of Φ50mm×100 mm are cut using a wire cutting machine. Use a polishing machine to polish the cross sections of both ends of the sample, ensuring that the parallelism error of the end faces is less than 0.05 mm, the smoothness error is less than 0.02 mm, and the diameter error is less than 0.3 mm. To reduce the influence of material heterogeneity, coal cores were selected based on similar physical properties. Specifically, samples with a density ranging from 1.35 to 1.40 g/cm³ and acoustic velocity between 2473 and 2772 m/s were retained. A total of 11 cores were excluded due to significant deviations from these criteria. This screening process ensured that the selected specimens were representative of the Benxi Formation deep coal and suitable for reliable mechanical testing.

Place the preferred coal sample in an oven with a constant temperature of 80 °C, dry it until the sample mass no longer changes, and then remove it. After the coal sample cools to room temperature, weigh it and record it as M_0. Soak the coal rock sample in a closed vacuum container filled with on-site drilling fluid, continuously record the mass of the coal sample under different water content states, M_S, and calculate the water content of the coal sample to obtain three groups of coal samples with different water contents. The water content W can be expressed as

$$W = \frac{M_s - M_0}{M_0} \times 100\% \tag{14}$$

Experimental apparatus and process

This experiment used a multi-field coupled triaxial testing system to explore the mechanical properties and damage evolution of deep coal rock under the coupling of thermal-hydro-mechanical forces. The maximum axial pressure of the device is 150 MPa, the maximum confining pressure is 15 MPa, and the maximum temperature is 150℃. The schematic diagram of the experimental device is shown in Fig. 4. The device can automatically and intelligently apply confining and axial pressure and can achieve closed-loop servo control for real-time monitoring of temperature and pressure, real-time data processing, and data collection.

The specific experimental steps are as follows: (1) Apply silicone rubber evenly to the surface of the coal sample after soaking in drilling fluid, and place the coal sample at the bottom of the triaxial pressure chamber after drying. A cylindrical heat-shrink tube is used to cover the coal sample tightly, and it is secured with metal hoops at the upper and lower ends to ensure the test piece's air tightness. Finally, connect the remaining auxiliary equipment in order according to the installation sequence; (2) Check the air tightness of the triaxial pressure chamber and various pipelines, and then perform vacuum degassing on the device; (3) Slowly adjust the inlet valve and inject the collected coal rock gas into the triaxial pressure chamber. After the pore pressure reaches 2 MPa, maintain the valve opening and fully adsorb for 48 h until the coal sample reaches adsorption equilibrium; (4) Set the experimental temperature and pressure conditions according to the actual temperature and pressure environment downhole; (5) Triaxial compression failure experiments were conducted under predefined conditions of temperature, confining pressure, pore pressure, and axial pressure. Axial loading was applied continuously at a constant rate of 0.1 mm/min. Throughout the loading process, the axial pressure was maintained higher than the confining pressure. The experiment automatically terminated upon complete failure

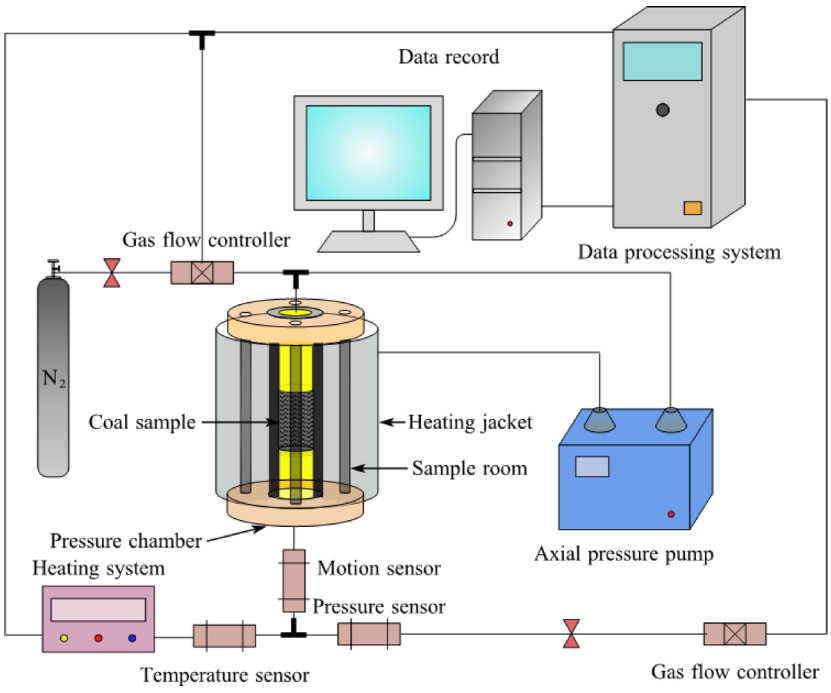

Fig. 4. Structure diagram of multi-field coupling triaxial test system.

No.	σ_3/MPa	T/℃	W/%
1	0	25	0
2	5	25	0
3	10	25	0
4	15	25	0
5	0	25	0
6	0	60	0
7	0	90	0
8	0	120	0
9	0	25	0
10	0	25	2
11	0	25	4
12	0	25	6

Table 2. Experimental parameters.

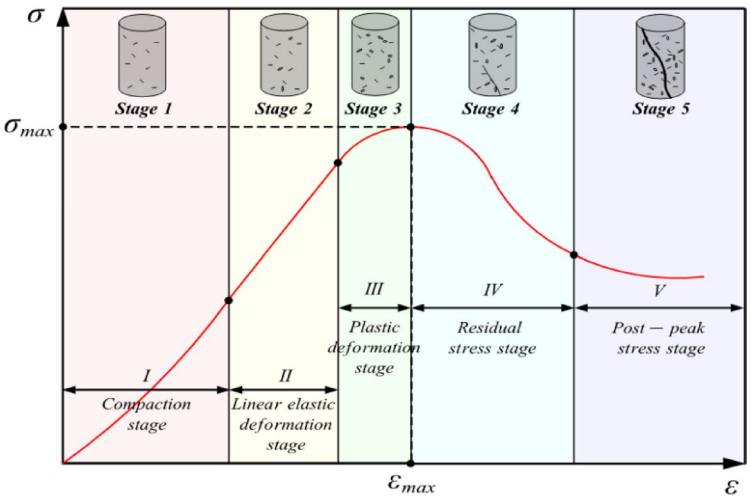

Fig. 5. Stage division diagram of stress-strain curve.

of the coal rock, during which all experimental data were recorded and collected; (6) Replace the coal sample, reset the temperature, and confining pressure, and repeat the above operations.

Table 2 is a table of experimental parameters to ensure that the triaxial test covers the interaction between temperature, water content, and confining pressure, while meeting the mechanical parameters required for the THM damage constitutive model.

Considering the operational limits of the experimental apparatus and the practical relevance to field conditions, the temperature and confining pressure ranges adopted in this study were selected based on representative values observed in typical deep coalbed methane reservoirs in China. While not reaching the maximum values at depths > 2000 m, these conditions are sufficient to simulate the dominant thermos-hydro-mechanical coupling effects encountered in deep formations. The results obtained under these conditions provide a reliable basis for developing and validating the proposed damage model. Furthermore, the proposed damage model exhibits parameter scalability, allowing the experimental results to reasonably reflect the mechanical responses and damage evolution of deep coal rocks under coupled THM conditions.

Experimental results

Stress-strain characteristics

Based on the selected experimental data, a schematic diagram of the stress-strain curve is drawn, as shown in Fig. 5. The stress-strain curve of triaxial compression can be divided into five stages: compaction stage, elastic deformation stage, plastic deformation stage, post-peak stress drop stage, and residual strength stage[33,34]. Under axial compression loading, the primary fractures and pores of the rock mass are subjected to certain compaction, resulting in an upward trend in the stress-strain curve, which is called the compaction stage. When the primary fractures and pores in the rock mass are fully compacted, the stress-strain enters the elastic deformation stage, during which the coal rock has elastic deformation characteristics and obeys the Hock law. As the axial stress is loaded, the volumetric strain of the rock mass slowly increases, but the elastic modulus slowly decreases, causing the development and expansion of micro-cracks. This stage is called the plastic deformation stage. The

compaction stage, elastic deformation stage, and plastic deformation stage are collectively referred to as the pre-peak stage. During this stage, the stress-strain curve is approximately linear, and the rock mass has the characteristics of elastic deformation. The micro-cracks further expand and extend until they interpenetrate to form macroscopic fractures, resulting in maximum cumulative damage. The rock mass is subjected to shear failure, releasing elastic energy, and the axial stress drops significantly, resulting in a stress drop phenomenon. This stage is called the post-peak stress drop stage. The damaged coal rock still has a certain bearing capacity, and its internal structural concave and convex parts continue to wear or shear, with cracks compacted and closed, resulting in a significant deformation after reaching residual strength. This stage is called the residual strength stage.

Figure 6 shows the stress-strain curves of coal rocks under different confining pressures, temperatures, and moisture contents. As shown in Fig. 6(a), comparing the stress-strain curves of coal rocks under different confining pressures, it can be found that there are some differences in the characteristics of deformation and failure laws of coal rocks under different confining pressures. As the confining pressure increases, the peak strength increases, and the corresponding curve in the pre-peak stage becomes steeper, which means that the compressive strength and elastic modulus increase. The presence of confining pressure can compact the original fractures and pores in the rock mass, hindering their initiation, expansion, and extension. Therefore, the increase in confining pressure will enhance the ability of coal rocks to resist deformation and failure, and the peak strength and elastic modulus of the rock mass will increase accordingly.

As shown in Fig. 6(b), comparing the stress-strain curves of coal rock at different temperatures, it can be found that temperature significantly impacts the stress-strain characteristics of coal rock. As the temperature increases, the peak strength decreases, and thermal expansion and thermal cracking reduce the bearing capacity of coal rock, which gradually exhibits certain ductile characteristics. The thermal stress generated by temperature is greater than the external stress, and the expansion of coal matrix leads to a reduction in pore and fracture space. However, as the temperature increases, the microscopic cracks inside the coal rock continue to sprout and expand, and the elastic modulus of coal rock decreases.

As shown in Fig. 6(c), comparing the stress-strain curves of coal rocks under different moisture contents, it can be found that there are significant differences in the stress-strain characteristics under different moisture contents. Under the same immersion system, the increase in moisture content causes the corresponding compression stage interval of the stress-strain curve of coal rocks to increase, while the elastic deformation stage shrinks and the peak strength decreases. The post-peak characteristics of the stress-strain curves of coal rocks with different moisture contents are different, and their failure trends mainly include three types: steady decline, linear decline, and stepwise decline. As the moisture content increases, the post-peak curve characteristics gradually change from approximately vertical linear decline to stepwise decline, and then gradually transition

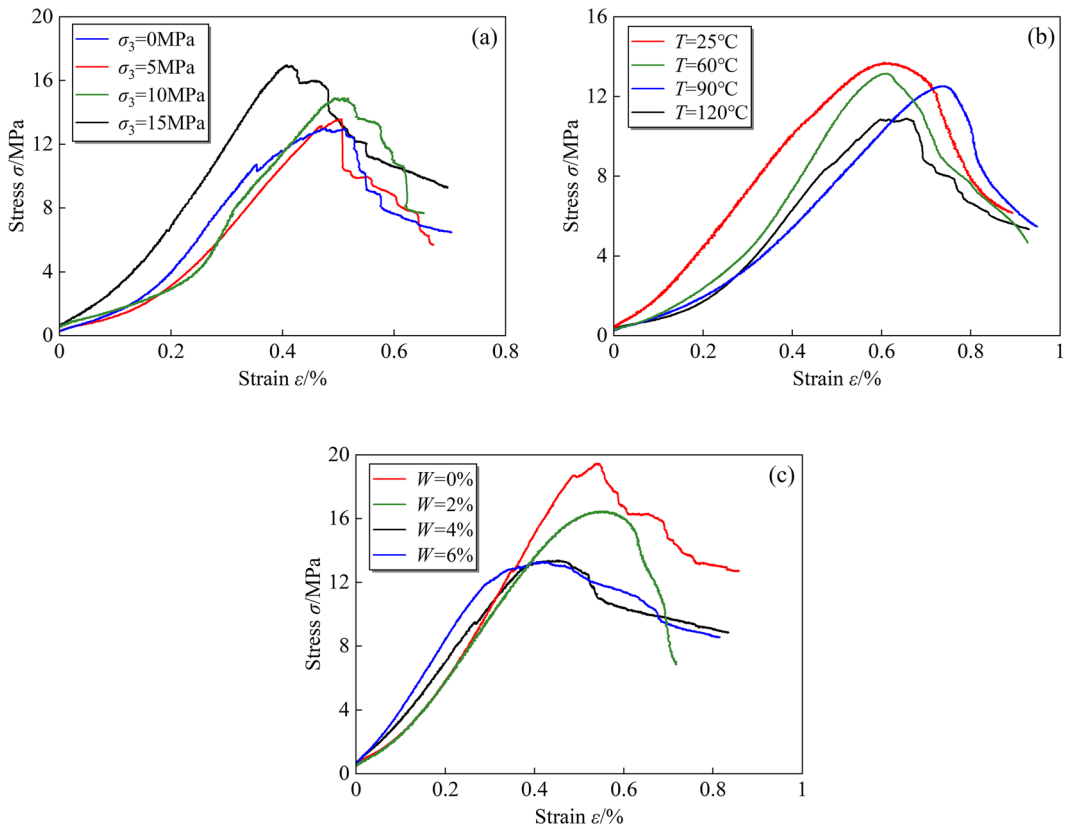

Fig. 6. Stress-strain curves under different experimental conditions.

to steady decline. The main reasons for this phenomenon are as follows: (1) The invasion of drilling fluid filtrate into rock fractures weakens the cohesion between matrix particles and between matrix and clay minerals, reducing the peak strength and elastic modulus of the rock mass and deteriorating its mechanical properties. (2) The continuous expansion of clay minerals and the gradual dissolution of soluble salts weaken the cementation effect of weak-surface structures, resulting in a decrease in the bearing capacity of the rock mass and an increase in plastic deformation of coal rocks.

Mechanical characteristics analysis

In the triaxial compression test, the deformation and failure process of coal rock is usually divided by crack closure stress, crack initiation stress, crack damage stress and peak stress[15,35]. The crack closure stress is the stress corresponding to the compaction stage, and the crack initiation stress represents the stress at the beginning of the microcrack, which is the termination stress of the compaction stage and the initial stress of the elastic deformation stage. The crack damage stress is the termination stress of the elastic deformation stage and the initial stress of the plastic deformation stage. The peak stress is the termination stress during the plastic deformation stage, and also the stress corresponding to the highest point of the stress-strain curve. Figure 7 shows the variation patterns of peak stress and crack closure stress of coal rock with increasing confining pressure, temperature, and water content. Figure 8 shows the variation of the elastic modulus and initial deformation modulus of coal rock with increasing confining pressure, temperature, and moisture content. The initial deformation modulus refers to the elastic modulus of coal rock at the onset of deformation, before the initiation of any significant damage or microcrack development, and is defined as the slope of the line connecting the origin to the first data point on the stress–strain curve.

As the confining pressure increases, the primary fractures and pores within the coal rock close, enhancing the resistance of the coal rock to deformation to some extent. As shown in Fig. 7(a), the peak stress and crack closure stress of the coal rock increase exponentially with the increase in confining pressure. The closure stress and peak stress of the coal rock under no confining pressure are 4.80 MPa and 11.70 MPa, respectively. Under confining pressures of 0, 5, 10, and 15 MPa, the crack closure stress of the coal rock increases by 7.41%, 16.57%, 35.09%, and 59.04%, respectively, and the peak stress increases by 5.98%, 11.97%, 29.06%, and 43.59%, respectively. As shown in Fig. 8(a), the elastic modulus and initial deformation modulus of the coal rock increase exponentially with the increase in confining pressure. Under no confining pressure, the initial deformation modulus and elastic modulus of the coal rock are 1.34 GPa and 3.60 GPa, respectively. Under confining pressures of 0, 5, 10, and 15 MPa, the initial deformation modulus of the coal rock increases by 4.48%, 5.97%, 10.45%, and 20.90%, respectively, and the elastic modulus increases by 2.22%, 2.78%, 4.167%, and 8.06%, respectively.

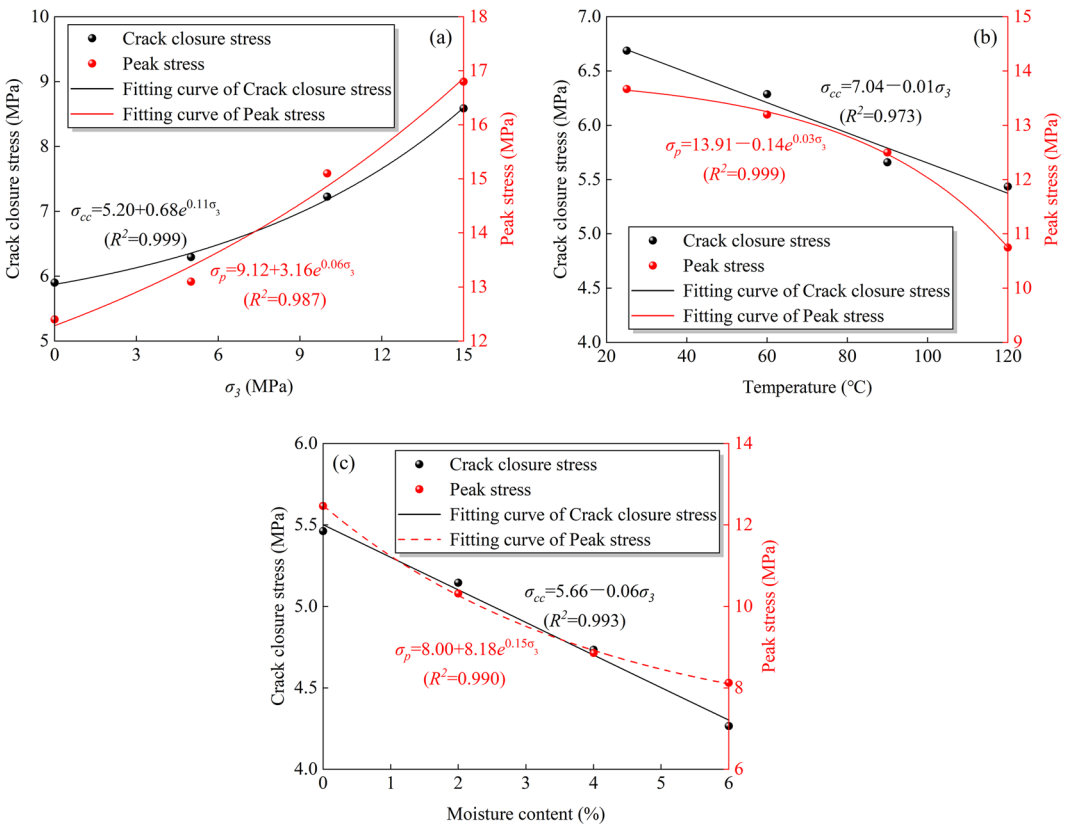

Fig. 7. Variation of peak stress and crack closure stress.

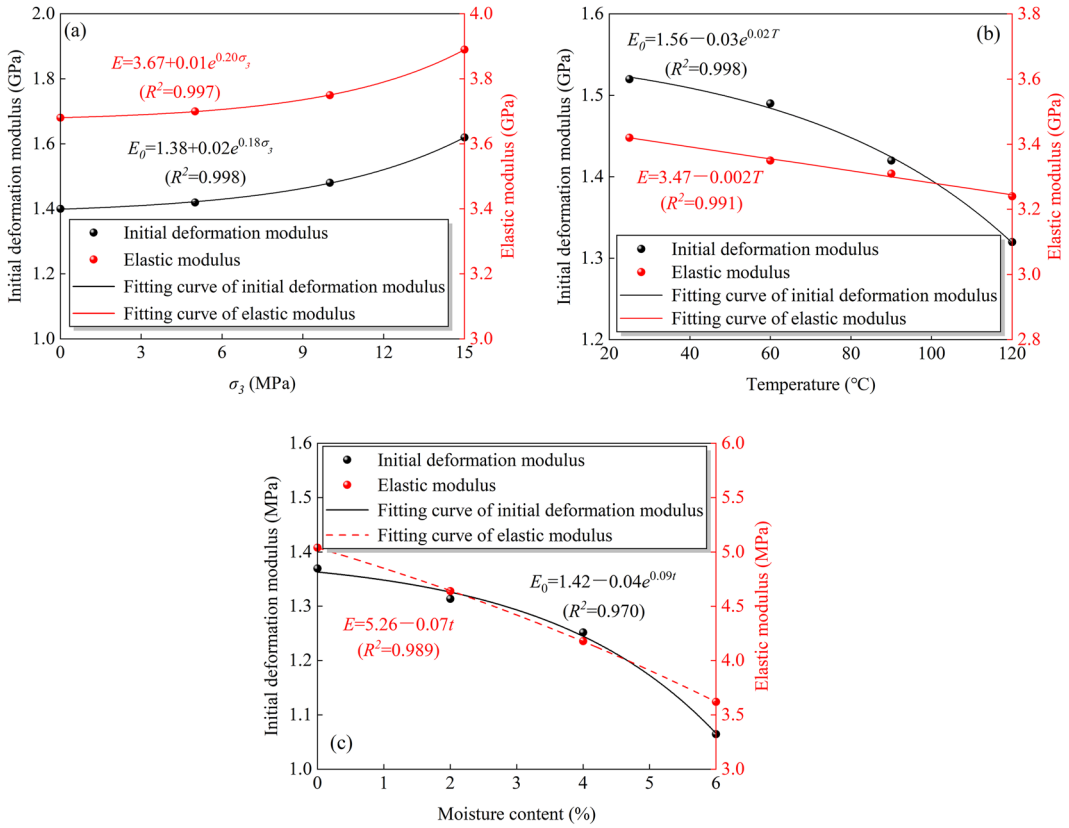

Fig. 8. The variation law of elastic modulus and initial deformation modulus.

As the temperature increases, thermal expansion and thermal cracking cause thermal damage to coal rock under temperature effects, resulting in changes in mechanical properties. As shown in Fig. 7(b), the peak stress decreases exponentially with increasing moisture content, while the crack closure stress decreases linearly with increasing moisture content. At 25 °C, the closure stress and peak stress of coal rock are 6.69 MPa and 13.67 MPa, respectively. At 60 °C, 90 °C, and 120 °C, the crack closure stress of coal rock decreases by 5.99%, 15.37%, and 18.74%, respectively, while the peak stress decreases by 3.45%, 8.57%, and 21.36%, respectively. As shown in Fig. 8(b), the elastic modulus and initial deformation modulus of coal rock decrease linearly and exponentially with increasing temperature. At 25 °C, the initial deformation modulus and elastic modulus of coal rock are 1.52 GPa and 3.42 GPa, respectively. At 60 °C, 90 °C, and 120 °C, the initial deformation modulus of coal rock decreases by 1.28%, 6.58%, and 13.16%, respectively, while the elastic modulus decreases by 2.05%, 3.22%, and 5.26%, respectively.

With the increase of moisture content, the clay minerals and soluble salts in coal rock dissolve, hydrate and expand, and micro-pores and cracks continue to sprout and expand, resulting in serious deterioration of mechanical properties. As shown in Fig. 7(c), the peak stress decreases exponentially with the increase of moisture content, and the crack closure stress decreases linearly with the increase of moisture content. The crack closure stress and peak stress of dry coal rock are 5.65 MPa and 12.87 MPa, respectively. Under the conditions of moisture content of 2%, 4%, and 6%, the crack closure stress of coal rock decreases by 8.92%, 16.21%, and 24.34%, respectively, and the peak stress decreases by 19.84%, 31.19%, and 36.15%, respectively. As shown in Fig. 8(c), the elastic modulus and initial deformation modulus of coal rock decrease linearly and exponentially with the increase of moisture content. The initial deformation modulus and elastic modulus of dry coal rock are 1.39 GPa and 5.52 GPa, respectively. Under the conditions of moisture content of 2%, 4%, and 6%, the initial deformation modulus of coal rock decreases by 6.87%, 10.25%, and 23.66%, respectively, and the elastic modulus decreases by 15.94%, 24.28%, and 34.42%, respectively.

Failure characteristics

Figure 9 shows the final macroscopic failure photos of coal rocks under different confining pressures, temperatures, and moisture contents. The red lines represent the macroscopic cracks on the surface of the coal rock, while the green lines represent the secondary cracks on the surface of the coal rock. It can be seen that as the confining pressure, temperature, and moisture content increase, the type and number of cracks on the surface of the coal rock change significantly.

Under the action of confining pressure, the ability of coal rock to resist deformation and failure is optimized, and their mechanical properties are improved. As shown in Fig. 9(a), under the action of four confining pressures, the surface of coal rock has obvious shear cracks running through the entire rock mass. Under the

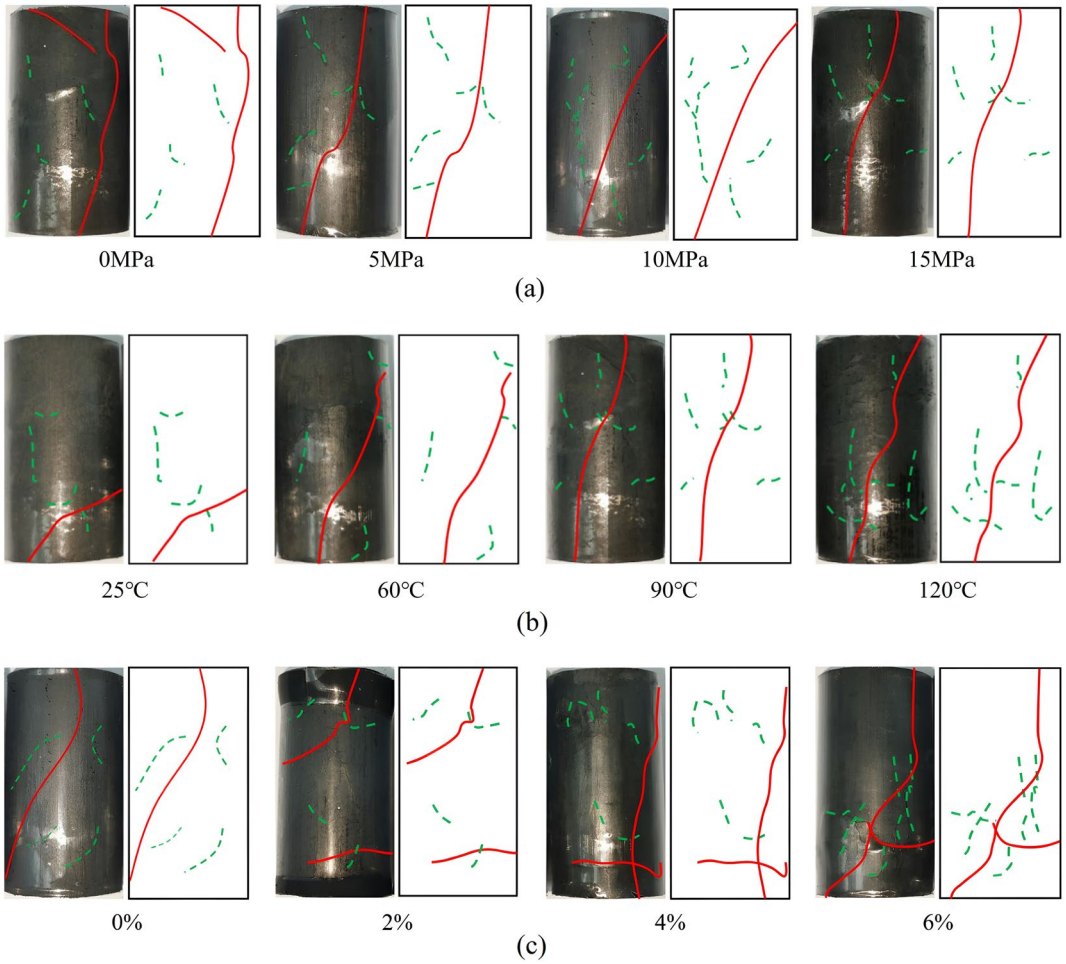

Fig. 9. Macroscopic failure photos of coal rock under different experimental conditions: (a) Different confining pressures; (b) Different temperatures; (c) Different water content.

action of 4 MPa confining pressure, the appearance of coal rock is complete, with no obvious matrix collapse phenomenon, and the failure mode presents tensile-shear conjugate failure; under the action of 3 MPa confining pressure, the surface of coal rock develops tensile cracks approximately parallel to the axis, and the failure mode is still tensile-shear conjugate failure; under the action of 2 MPa confining pressure, the failure characteristics of coal rock change from tensile-shear conjugate failure to single shear failure; under the action of 1 MPa confining pressure, there are two shear cracks that are perpendicular to each other and have obvious development, and the number of tensile cracks decreases.

Based on the previous analysis, it can be seen that temperature has a small but non-negligible effect on thermal damage to coal rock. An increase in temperature can lead to a certain degree of strength deterioration and an increased risk of instability. As shown in Fig. 9(b), with the increase in temperature, shear cracks gradually develop on the surface of coal rock, and local matrix collapse occurs. When the temperature is 120 °C, significant shear cracks appear on the surface of coal rock, penetrating throughout the entire rock mass, and tensile cracks connect and penetrate, resulting in the destruction of the overall structure.

Under the action of drilling fluid, the mechanical properties of coal rock weaken, leading to severe instability and failure of coal rock. As shown in Fig. 9(c), there are several tensile main fractures running through the matrix and approximately parallel to the axis in dry coal rock, which exhibit prominent single tensile failure characteristics. The coal rock produces local matrix shedding, and the shedding coal matrix is relatively fragmented. As the moisture content increases, the failure characteristics of coal samples shift towards tensile-shear conjugate failure, with a decrease in the number and length of tensile main fractures, an increase in the number, length, and inclination of shear secondary fractures distributed around them, and a more complete shedding of coal matrix. The shear failure trend gradually increases. When the failure characteristics of coal rock completely transform into single shear failure, with the increase of moisture content, the number of shear fractures running through the coal body continues to decrease, and the coal sample is relatively complete, with no obvious shedding of coal matrix.

Specifically, increasing temperature, moisture content, and decreasing confining pressure respectively lead to increases in the thermal damage variable (D_T), moisture-induced damage variable (D_w), and mechanical damage variable (D_M). These increases jointly contribute to the rise in the total damage variable (D), which

results in a notable reduction in the structural stiffness and tensile strength of the coal rock. As a consequence, the number of cracks increases, and crack propagation becomes more localized, ultimately driving a transition in macroscopic failure mode from tensile-shear conjugate failure to predominantly shear failure. This observed trend is consistent with the fracture patterns under different conditions in Fig. 9, confirming that the damage variables in our model effectively capture the evolution of failure mechanisms under varying thermal-hydro-mechanical conditions.

Model validations and discussion

Model validations

To comprehensively evaluate the accuracy and applicability of the proposed damage constitutive model, the following comparison and error analysis were conducted. Given the fundamental differences in environmental conditions and damage mechanisms, particularly the influence of drilling fluid immersion, a direct comparison with existing water-based damage models was not conducted; instead, the proposed model was quantitatively validated against experimental data obtained under the specific conditions of this study. The obtained damage statistical parameters were substituted into the damage variable expression (8) and the damage constitutive Eq. (13), and the stress-strain relationships under different confining pressures, temperatures, and moisture contents were fitted, and compared with the conventional triaxial compression experimental curves. Table 3 shows the parameter values taken for the coal rock damage constitutive model. Figure 10 ~ 12 are schematic diagrams of the comparison between the deep coal rock damage constitutive model under thermal-hydro-mechanical coupling and the experimental curves.

From the graph, it can be seen that during the initial application of axial stress, the pores and cracks inside the coal rock slowly close, and the damage variable gradually decreases. However, this compaction effect is considered a reversible physical process and is therefore not reflected as a decrease in the damage variable in our model. As a result, the damage curve begins with a slow increase rather than an initial reduction. When the pores and fractures are completely closed, the coal rock transforms from a primary porous and high porosity rock mass to a dense rock mass, and the damage variable is approximately 0. Then, in the process of axial compression loading, the primary cracks and pores of coal rock began to expand, and the new micro cracks began to sprout, expand and split. The damage of coal rock rapidly accumulated, and the damage variable continued to increase. Primary cracks, pores, and newly formed micro cracks continue to expand, split, and connect until penetrating macro cracks are formed, causing damage to the macroscopic structure of coal rock. When the coal rock is completely destroyed, the cumulative damage variable is approximately 1.

For the pre-peak stage, the theoretical curves and experimental curves for the compaction stage and plastic deformation stage are basically in complete agreement, while there are some differences between the theoretical curves and experimental curves for the elastic deformation stage, but the curve trends have excellent matching. The axial strain increases linearly with the increase of stress, and the peak stress and peak strain values are basically consistent. For the post-peak stress drop stage and residual stress stage, as the axial stress increases, both the theoretical curves and experimental curves show a rapid downward bending and extension trend after reaching the peak, with a lower fitting accuracy compared to the pre-peak stage, but the trends are basically consistent.

Furthermore, the error between the experimental results and the theoretical values calculated by the model is analyzed. The last two columns of the table provide the detailed percentage errors, as shown in Table 4. According to the error percentages, all calculated errors of the proposed model are within 10%, demonstrating a high level of accuracy.

In summary, the deep coal damage constitutive model established in this paper, which considers the coupling effects of thermal-hydro-mechanical, has good rationality and feasibility, and can better reflect the strength variation characteristics, deformation failure characteristics, and damage evolution characteristics of coal under different temperatures, confining pressures, and moisture contents.

σ_3/MPa	T/℃	W/%	E/GPa	λ	u	q	*n*	ε_p/%	σ_p/MPa	ε_{cr}/%
0	25	0	3.68	0.32	0.20	0.8	6	0.47	12.4	0.54
5	25	0	3.71	0.25	0.25	0.8	5	0.49	13.2	0.56
10	25	0	3.77	0.40	0.30	0.8	4	0.48	15.3	0.55
15	25	0	3.88	0.31	0.35	0.8	5	0.42	16.8	0.56
0	25	0	3.39	0.30	0.20	0.8	6	0.60	13.7	0.77
0	60	0	3.30	0.28	0.25	0.8	7	0.62	13.1	0.72
0	90	0	3.28	0.35	0.30	0.8	4	0.74	12.4	0.81
0	120	0	3.24	0.40	0.35	0.8	6	0.73	10.8	0.78
0	25	0	5.00	0.34	0.20	0.8	5	0.54	19.3	0.60
0	25	2	4.71	0.29	0.25	0.8	8	0.58	16.1	0.64
0	25	4	4.20	0.31	0.30	0.8	6	0.47	13.3	0.53
0	25	6	3.61	0.38	0.35	0.8	4	0.43	12.6	0.64

Table 3. Parameter values of coal rock damage constitutive model.

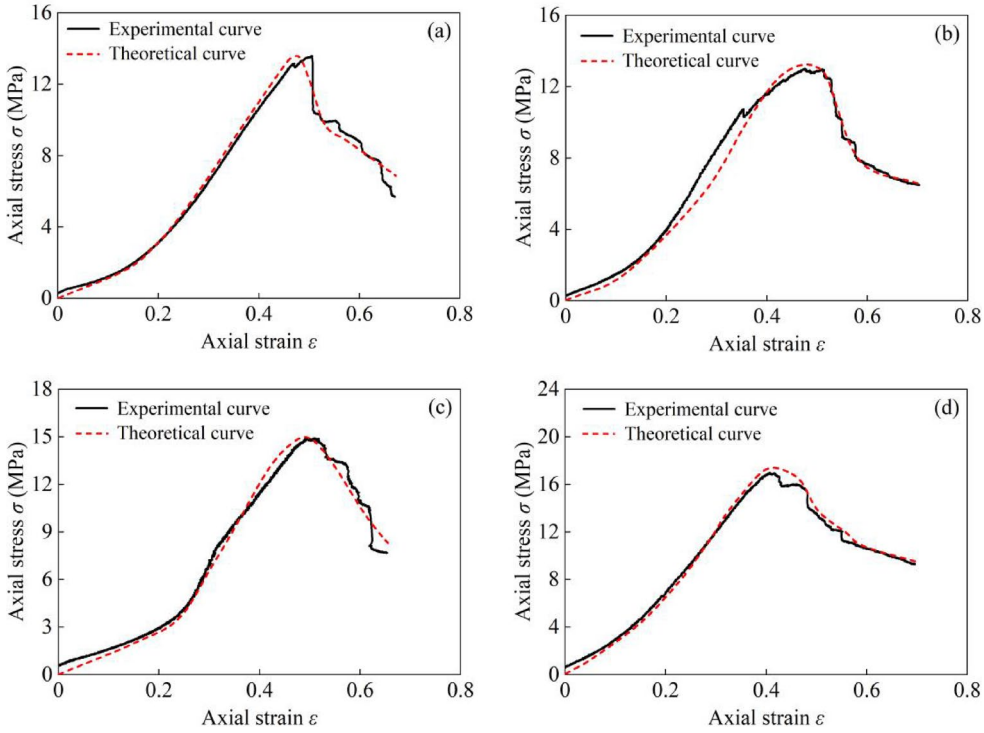

Fig. 10. Comparison of stress-strain experimental curves and theoretical curves of coal rock under different confining pressures; (**a**)$\sigma_3 = 0$ MPa; (**b**) $\sigma_3 = 5$ MPa; (**c**) $\sigma_3 = 10$ MPa; (**d**) $\sigma_3 = 15$ MPa.

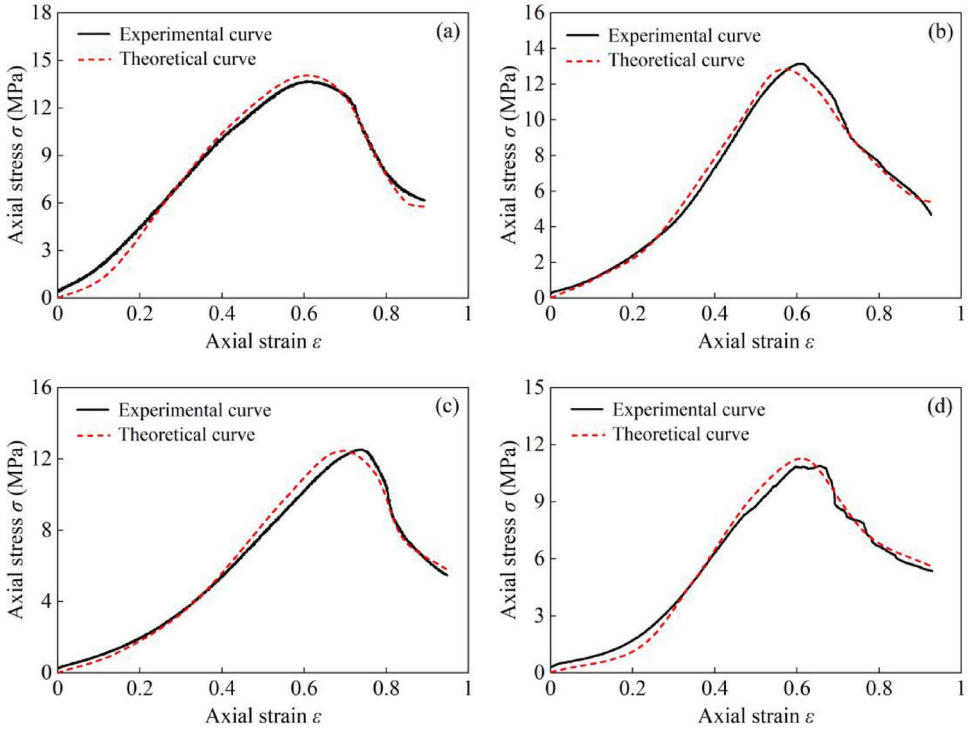

Fig. 11. Comparison of stress-strain experimental curves and theoretical curves of coal rock at different temperatures; (**a**) $T = 25$°C; (**b**) $T = 60$°C; (**c**) $T = 90$°C; (**d**) $T = 120$°C.

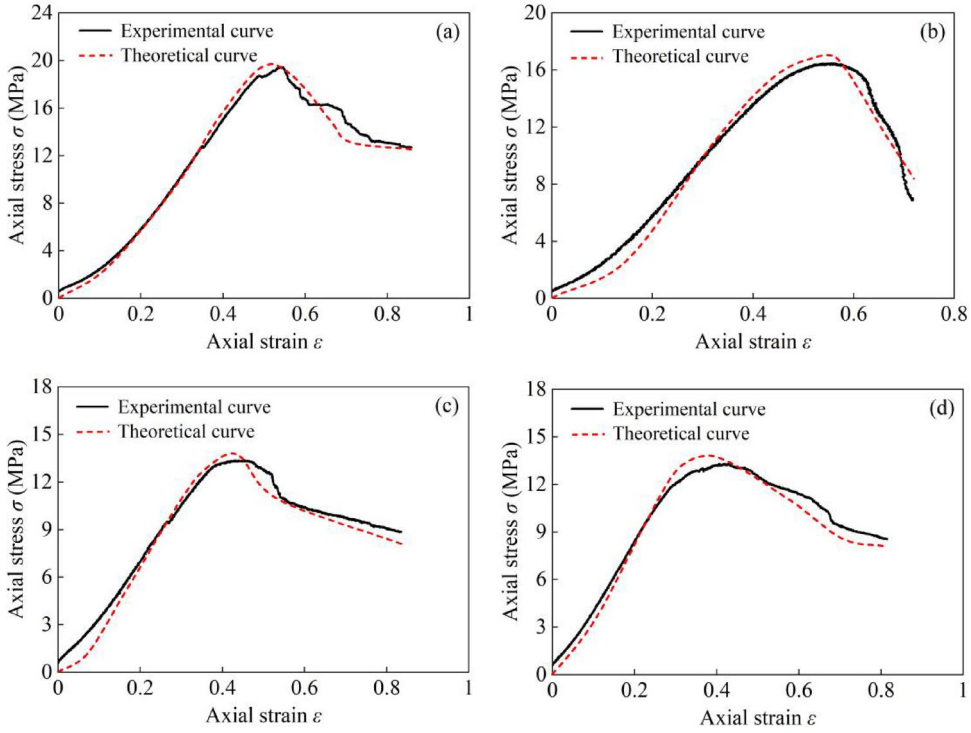

Fig. 12. Comparison of stress-strain experimental curve and theoretical curve of coal rock under different water content; (**a**) $W = 0\%$; (b) $W = 2\%$; (**c**) $W = 4\%$; (**d**) $W = 6\%$.

No.	Experimental results		Theoretical calculation results		Relative error/%	
	ε_p/%	σ_p/MPa	ε_p/%	σ_p/MPa	ε_p/%	σ_p/MPa
1	0.47	12.4	0.43	12.5	8.51	0.81
2	0.49	13.2	0.45	13.5	8.16	2.27
3	0.48	15.3	0.44	15.6	8.33	1.96
4	0.42	16.8	0.40	17.4	4.76	3.57
5	0.60	13.7	0.57	14.2	5.00	3.65
6	0.62	13.1	0.57	12.6	8.06	3.82
7	0.74	12.4	0.67	12.3	9.46	0.81
8	0.73	10.8	0.67	11.8	8.22	9.26
9	0.54	19.3	0.50	19.9	7.41	3.11
10	0.58	16.1	0.53	16.9	8.62	4.97
11	0.47	13.3	0.43	14.1	8.51	6.02
12	0.43	12.6	0.39	13.6	9.30	7.94

Table 4. Comparison of experimental curve fitting results.

Discussion

Model parameter analysis

To further verify the feasibility and rationality of the model, the model parameters were analyzed. When the other parameters remain unchanged, the influence of parameters q and n on the mechanical response is shown in Fig. 13, and the influence on the damage variable is shown in Fig. 14. When the other parameters remain unchanged, parameter q mainly affects the shape of the post-peak curve by affecting the magnitude of residual stress, and also has a certain impact on peak strength. As parameter q decreases, the residual stress increases, and the post-peak curve shows a trend of slowing down before steepening, indicating a slower stress drop rate, reflecting the stress characteristics during the residual strain stage. When the other parameters remain unchanged, parameter n affects the shape of the post-peak stress drop curve by affecting the post-peak stress drop rate, reflecting the degree of deterioration of post-peak stress, with a small impact on peak strength, initial deformation modulus, and elastic modulus.

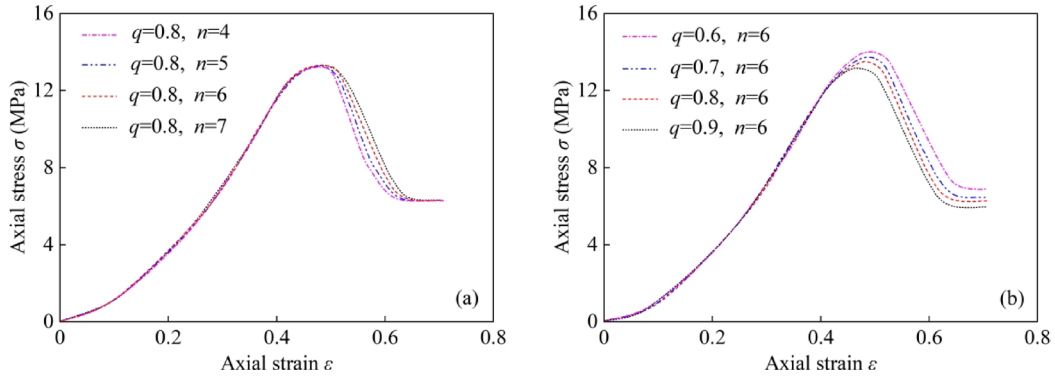

Fig. 13. The influence of model parameters on the stress-strain curve.

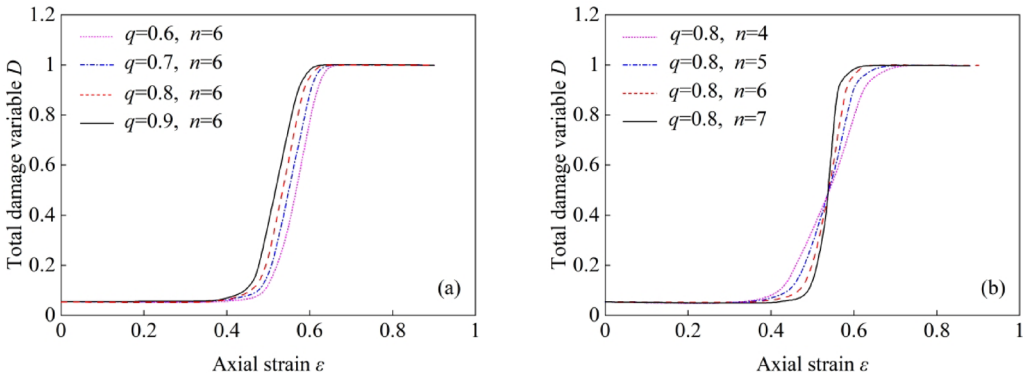

Fig. 14. The influence of model parameters on damage evolution.

In terms of physical interpretation, parameter q reflects the residual strength retention capacity of coal rock after peak stress. It is associated with the degree of matrix cohesion, mineral bonding strength, and macrostructural completeness, which collectively determine how much mechanical integrity the coal retains in the residual deformation stage. A lower q value corresponds to a higher residual stress and a more gradual stress drop, indicative of ductile behavior. Parameter n, on the other hand, governs the rate of damage accumulation during the post-peak stage. It reflects the sensitivity of the material to stress-induced microcrack propagation and is influenced by the heterogeneity of the coal matrix, the density and distribution of cleats, and the initial microfracture structure. A higher n implies a more brittle response, where damage localizes rapidly and stress drops sharply after reaching the peak. Together, these parameters not only control the shape of the stress-strain and damage evolution curves but also encapsulate key physical properties of the coal such as brittleness, and microstructural damage evolution behavior under complex loading conditions.

Characteristics of damage evolution

Based on experimental data, the total damage evolution curve of coal rock under different confining pressures, temperatures, and moisture contents was obtained through the calculation of a coupled thermal-hydro-mechanical deep coal rock damage constitutive model, as shown in Fig. 15. It can be seen that the variation trend of coal rock damage variables under different confining pressures, temperatures, and moisture contents is basically consistent, and the damage curve generally shows an "S-shaped" growth. The damage process of coal rock is similar to its stress-strain characteristics, and can also be divided into five stages: compaction stage, elastic deformation stage, plastic deformation stage, post-peak stress drop stage, and residual strength stage[11,36]. Figure 16 illustrates the schematic diagram of the coal rock damage evolution stages. Compaction and Elastic Deformation Stage: This corresponds to the nearly horizontal segment at the beginning of the damage evolution curve, where the damage variable remains almost constant. At this stage, rock fractures are compacted and closed without propagation, and the rock micro-elements undergo elastic deformation. Plastic Deformation Stage: This corresponds to the concave upward portion of the damage evolution curve, where the damage variable increases rapidly. During this stage, fractures begin to propagate at an accelerating rate, and the rock undergoes plastic yielding. Post-Peak Stress Drop Stage: This corresponds to the convex upward segment of the damage evolution curve, where the slope gradually decreases. Fractures continue to expand and coalesce, leading to a gradual loss of rock strength. Residual Deformation Stage: At this stage, macroscopic fracture surfaces form within the rock, resulting in complete structural failure. The damage variable approaches 1 and remains constant thereafter.

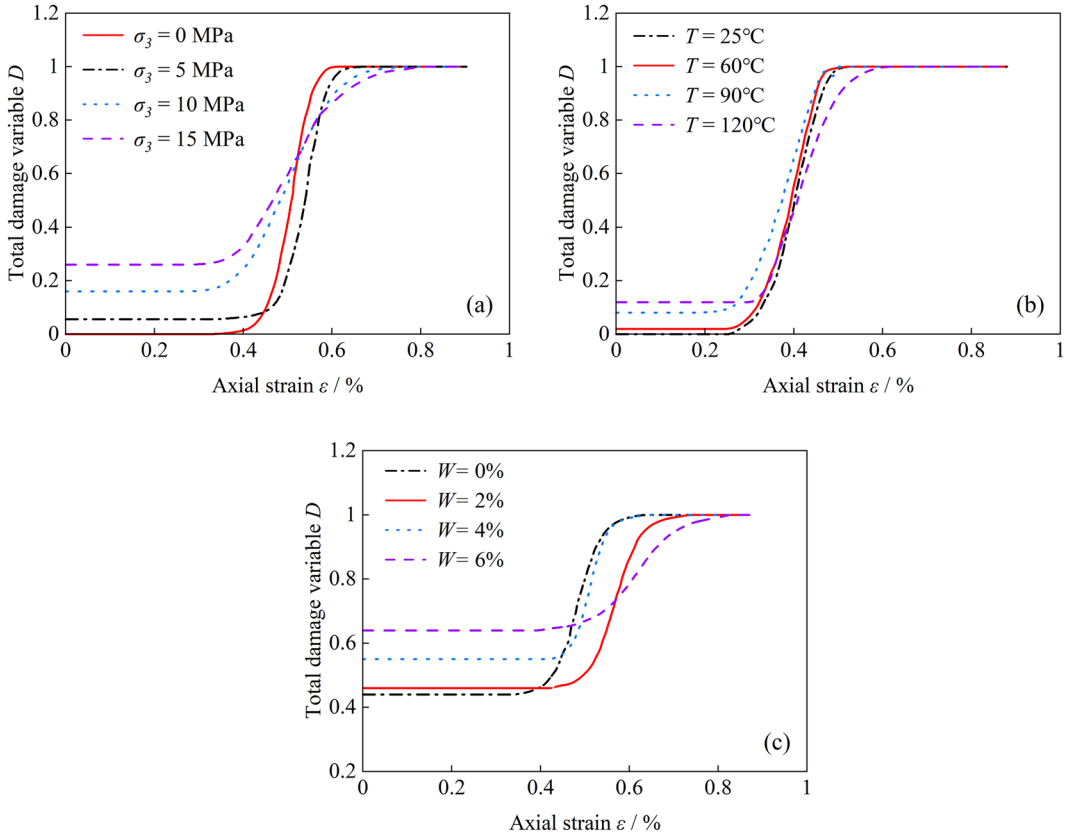

Fig. 15. Damage evolution curve.

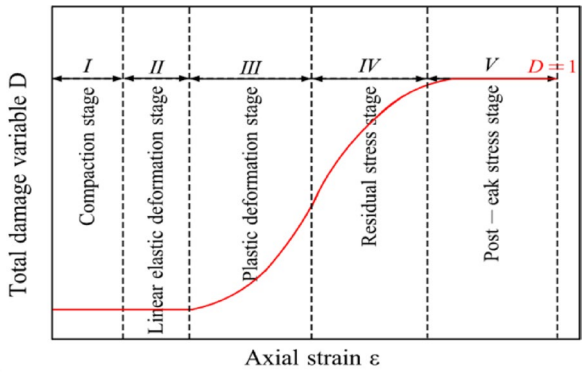

Fig. 16. Schematic diagram of coal rock damage evolution stages.

As shown in Fig. 15(a), the damage evolution curve of coal rock under different confining pressures also exhibits an S-shaped shape and gradually increases. As the confining pressure increases, the internal pores and fractures of coal rock close, the porosity of coal rock decreases, the resistance to deformation increases, and the damage deformation of coal rock decreases.

As shown in Fig. 15(b), the damage variable of coal rock at different temperatures increases with the increase of temperature, and the internal skeleton of coal rock expands, and the pores and cracks expand and extend. The higher the temperature, the more serious the damage to coal rock. Compared with confining pressure and moisture content, temperature has a more minor impact on coal rock damage, so it is recommended to weaken the role of temperature when studying coal rock damage under non-high temperature conditions.

As shown in Fig. 15(c), the initial damage of coal rock varies with different moisture contents. The higher the moisture content, the greater the initial damage. The initial damage of coal rock at four moisture contents of 0%, 2%, 4%, and 6% is 0.44, 0.46, 0.55, and 0.64, respectively. The crack initiation strain and initial damage variables of coal rock at the four moisture contents are basically equal, mainly due to the fact that during the compaction stage and elastic deformation stage, the coal rock mainly undergoes elastic deformation, and the

pores and fractures of the coal rock are in a closed state. When the external load reaches the crack initiation stress, the pores and fractures begin to extend and develop, and mechanical damage occurs in the rock mass. As the external load increases, mechanical damage continues to act on the coal body, and the amount of damage accumulates continuously, eventually reaching the final damage amount of 1. During mechanical damage to coal rock, as the moisture content increases, the strain gradually increases, the time required to reach the total damage amount increases, the plastic properties increase, and the total damage amount gradually decreases.

It is worth noting that the initial total damage value (D) ranges from 0.44 to 0.64, even under conditions of 0% moisture and low strain. This phenomenon does not contradict the model assumption that $D_M = 0$ for dry conditions. In our framework, D_M specifically denotes loading-induced mechanical damage, which is assumed to initiate after external stress application. However, the observed initial damage primarily originates from the intrinsic microstructural heterogeneity of the coal, including pre-existing pores, cleats, and microcracks, which exist prior to loading and are independent of both mechanical and moisture effects. Therefore, the initial damage state is incorporated into the model as a baseline condition reflecting inherent weakness of the material.

Conclusion

This paper takes the deep coal rock of the Benxi Formation in the Ordos Basin as the research object and, through multi-field coupled triaxial compression experiments under different temperatures, stress states, and moisture content conditions, studies the stress-strain characteristics, mechanical properties, and failure characteristics of deep coal rock under the coupling of thermal-hydro-mechanical forces. It also discusses the effects of temperature, stress state, and moisture content on the mechanical properties and damage characteristics of deep coal rock. Based on the Lemaitre strain equivalence hypothesis, a constitutive model containing the thermal-hydro-mechanical coupling damage evolution equation of deep coal rock is established, and the main conclusions are as follows:

(1) Based on the Lemaitre strain equivalence hypothesis, continuum damage mechanics, and thermodynamics, the damage constitutive coefficient, and damage correction coefficient are introduced as variables for investigation. The damage variables of deep coal rock under the action of confining pressure, temperature, and drilling fluid are defined, and a damage constitutive model for deep coal rock under the coupling of thermal-hydro-mechanical forces is established.

(2) Triaxial compression experiments on coal rock were conducted using a multi-field coupled triaxial testing system to investigate the stress-strain characteristics, mechanical properties, and failure characteristics during the failure process of coal rock. Drilling fluid immersion significantly degrades mechanical parameters such as peak stress and elastic modulus of coal rock, with certain time effects and non-uniformity. As the moisture content increases, the peak stress and elastic modulus of coal rock decrease to varying degrees, and the overall degree of deterioration increases, but the deterioration effect continues to weaken. The macroscopic failure mode of coal rock is mainly brittle failure dominated by shear and tension. As the confining pressure decreases and the moisture content increases, the failure mode of coal rock during loading changes from tensile-shear conjugate failure to single-shear failure.

(3) Through comparative analysis of the values of parameters q and n in the damage constitutive model established in this paper, parameter q reflects the residual deformation characteristics of coal rock after compression failure, while parameter n reflects the degree of weakening in the post-peak stage of the stress-strain curve. Therefore, the shape and trend of the damage evolution curve obtained from this model are mainly determined by q and n together.

(4) The final theoretical calculation curve of the model established in this paper is in good agreement with the experimental curve, which verifies the validity, rationality, and reliability of the model. The model can better reflect the deformation law, damage evolution characteristics, and instability failure mechanism of the deep coal rock stress-strain process with changes in confining pressure, temperature, and moisture content.

Data availability

All data, models, and code generated or used during the study appear in the submitted article.

Received: 14 May 2025; Accepted: 4 July 2025
Published online: 11 August 2025

References

1. Jianping, Y. E., Songyi, H. O. U. & Shouren, Z. H. A. N. G. Progress of coalbed methane exploration and development in China during the 13th Five-Year plan period and the next exploration direction. *Coal Geol. Explor.* **50** (3), 3. https://doi.org/10.12363/issn.1001-1986.21.12.0738 (2022).
2. Dehua, Z. H. O. U., Gang, C. H. E. N., Zhenlong, C. H. E. N. & Zengqin, L. Exploration and development progress, key evaluation parameters and prospect of deep CBM in China. *Nat. Gas. Ind.* **42** (6), 43–51. https://doi.org/10.3787/j.issn.1000-0976.2022.06.004 (2022).
3. Xujie, G. U. O. et al. Discovery and significance of coal measure gas in Junggar basin. *China Petroleum Explor.* **26** (6), 38. https://doi.org/10.3969/j.issn.1672-7703.2021.06.003 (2021).
4. Zhe, Z. H. A. O. et al. Geological characteristics and exploration breakthroughs of coal rock gas in carboniferous Benxi formation, Ordos basin, NW China. *Pet. Explor. Dev.* **51** (2), 262–278. https://doi.org/10.11698/PED.20230679 (2024).
5. Guangzhi, Y. I. N., Dengke, W. A. N. G., Dongming, Z. H., A., N. G. & Weizhong, W. A. N. G. Test analysis of deformation characteristics and compressive strengths of two types of coal specimens containing gas. *Chin. J. Rock. Mech. Eng.* **28** (2). https://doi.org/10.3321/j.issn:1000-6915.2009.02.027 (2009).
6. Jie, Y. U., Xiaohui, L. I. U. & Qijun, H. A. O. Acoustic emission characteristics and damage evolution of coal-rock under different confining pressures. *Coal Geol. Explor.* **48** (3), 20. https://doi.org/10.3969/j.issn.1001-1986.2020.03.019 (2020).
7. Xingping, L. A. I. et al. Multi-scale damage evolution characteristics of coal and rock under hydraulic coupling. *Chin. J. Rock Mechan. Eng.* **39** (S2), 3217–3228. https://doi.org/10.13722/j.cnki.jrme.2019.0921 (2020).

8. Enxiao, Y. U., Litao, M. A. & Fushuang, Z. H. O. U. Study on effects of drilling fluids on the mechanical properties of high-rank coal rock. *Coal Sci. Technol.* **48** (S1), 71–74. https://doi.org/10.13199/j.cnki.cst.2018.00722 (2020).
9. Bobo, L. I. et al. N. G., Experimental study on damage and the permeability evolution process of methane-containing coal under different temperature conditions. *J. Pet. Sci. Eng.* **184**, 106509. (2020). https://doi.org/10.1016/j.petrol.2019.106509
10. Bobo, L. I. et al. Mechanical properties and damage constitutive model of coal under the coupled hydro-mechanical effect. *Rock. Soil. Mech.* **42** (2), 2, 315–323. https://doi.org/10.16285/j.rsm.2020.5848 (2021).
11. Yao, Z. H. A. N. G. et al. E. N., N. G. Study on triaxial compression damage evolution characteristics of coal based on energy dissipation. *Chin. J. Rock Mech. Eng.*, **40**(8), 1614–1627. (2021). https://doi.org/10.13722/j.cnki.jrme.2020.1133
12. Yanan, G. A. O. et al. Mechanical properties and finite deformation behavior of coal under temperature, confining pressure and gas pressure. *J. China Coal Soc.* **46** (03), 898–911. https://doi.org/10.13225/j.cnki.jccs.yt21.0156 (2021).
13. Liqiang, Y. U. et al. Experimental study on the moisture migration and triaxial mechanical damage mechanisms of water-bearing coal samples. *Int. J. Rock Mech. Min. Sci.* **160**, 105263. https://doi.org/10.1016/j.ijrmms.2022.105263 (2022).
14. Jiale, F. U. et al. Experimental study on permeability and mechanical properties of coal under different pore pressure and confining pressure. *Coal Sci. Technol.* **51** (8), 150–159. https://doi.org/10.13199/j.cnki.cst.2022-0568 (2023).
15. Penghua, H. A. N. et al. A. N. G., Progressive damage characteristics and damage constitutive model of coal samples under long-term immersion. *Chin. J. Rock Mech. Eng.*, **43**(4), 918–933. (2024). https://doi.org/10.13722/j.cnki.jrme.2023.0495
16. Gaofei, D. A. I., Guangzhi, Y. I. N. & Wenli, P. I. Research on damage constitutive model and evolution equation of coal under uniaxial compression. *J. Tongji Univ. (Natural Science) (China)*. **32** (8), 986–989. https://doi.org/10.3321/j.issn:0253-374X.2004.08.002 (2004).
17. Guangzhi, Y. I. N., Dengke, W. A. N. G., Dongming, Z. H. A. N. G. & Zuoan, W. E. I. Endchronic damage constitutive model of coal containing gas. *Rock. Soil. Mech.* **30** (4), 885–889. https://doi.org/10.3969/j.issn.1000-7598.2009.04.004 (2009).
18. Guangzhi, Y. I. N. & Dengke, W. A. N. G. A coupled elastoplastic damage model for gas-saturated coal. *Chin. J. Rock Mechan. Eng.* **28** (5), 994–999. https://doi.org/10.3321/j.issn:1000-6915.2009.05.016 (2009).
19. Dengke, W. A. N. G., Guangzhi, Y. I. N., Jian, L. I. U., Fubiao, W. A. N. G. & Hu, Q. I. N. Elastoplastic damage coupled model for gas-saturated coal under triaxial compression. *Chinese Journal of Geotechnical Engineering*, **32**(1), 55–60. (2010). https://doi.org/CNKI:SUN:YTGC.0.2010-01-011
20. Ning, Z. H. A. N. G., Xiru, L. I., Hongmei, C. H. E. N. G. & Teng, T. E. N. G. A coupled damage-hydro-mechanical model for gas drainage in low-permeability coalbeds. *J. Nat. Gas Sci. Eng.* **35**, 1032–1043. https://doi.org/10.1016/j.jngse.2016.09.050 (2016).
21. Shaobin, H. U., Enyuan, W. A., N., G. & Xiaofei, L. I. U. Effective stress of gas-bearing coal and its dual pore damage constitutive model. *Int. J. Damage Mech.* **25** (4), 468–490. https://doi.org/10.1177/1056789515604372 (2016).
22. Wancheng, Z. H. U., Liyuan, L. I. U., Jishan, L. I. U., Chenhui, W. E. I. & Yan, P. E. N. G. Impact of gas adsorption-induced coal damage on the evolution of coal permeability. *Int. J. Rock Mech. Min. Sci.* **101**, 89–97. https://doi.org/10.1016/j.ijrmms.2017.11.007 (2018).
23. Xin, D. I. N. G. et al. Study on mechanical constitutive relationship and damage evolution of gas-bearing coal based on initial pore-cracks. *Mater. Rep.* **35**, 18096–18103. https://doi.org/10.11896/cldb.20080083 (2021).
24. Zhanglei, F. A. N. et al. A. N. G., Shuaishuai L. I. A. N. G., Non-Darcy thermal-hydraulic-mechanical damage model for enhancing coalbed methane extraction. *J. Nat. Gas. Sci. Eng.* **93**, 104048. (2021). https://doi.org/10.1016/j.jngse.2021.104048
25. Huilin, D. E. N. G., Hongwei, Z. H., O., U. & Lifeng, L. I. Fractional creep model of temperature-stress-time coupled damage for deep coal based on temperature-equivalent stress. *Results Phys.* **39**, 105765. https://doi.org/10.1016/j.rinp.2022.105765 (2022).
26. Feng, D. U. et al. Damage characteristics of coal under different loading modes based on CT three-dimensional reconstruction. *Fuel* **310**, 122304. https://doi.org/10.1016/j.fuel.2021.122304 (2022).
27. Pingping, Y. E. et al. Investigation on damage-permeability model of dual-porosity coal under thermal-mechanical coupling effect. *Gas Sci. Eng.* 205229. https://doi.org/10.1016/j.jgsce.2024.205229 (2024).
28. Rongxi, S. H. E. N., Xi, W. A. N. G., Hongru, L. I., Zhoujie, G. U. & Wei, L. I. U. Brittleness characteristics and damage evolution of coal under true triaxial loading based on the energy principle. *Nat. Resour. Res.* **33** (1), 421–434. https://doi.org/10.1007/S11053-023-10290-5 (2024).
29. Bobo, L. I. et al. Energy characteristics of coal or rock damage under thermo-mechanical coupling effect. *China Saf. Sci. J.* **29** (12), 91. https://doi.org/10.16265/j.cnki.issn1003-3033.2019.12.015 (2019).
30. Lemaitre, J. How to use damage mechanics. *Nucl. Eng. Des.* **80** (2), 233–245. https://doi.org/10.1016/0029-5493(84)90169-9 (1984).
31. Lisong, Z. H. A. N. G., Xiangzhen, Y. A. N., Xiujuan, Y. A. N. G. & Xinbo, Z. H. A. O. An analytical model of coal wellbore stability based on block limit equilibrium considering irregular distribution of cleats. *Int. J. Coal Geol.* **152**, 147–158. https://doi.org/10.1016/j.coal.2015.10.011 (2015).
32. Leilei, S. I. et al. The influence of long-time water intrusion on the mineral and pore structure of coal. *Fuel* **290**, 119848. https://doi.org/10.1016/j.fuel.2020.119848 (2021).
33. Kang, B. I. A. N. et al. Mechanical behavior and damage constitutive model of rock subjected to water-weakening effect and uniaxial loading. *Rock Mech. Rock Eng.* **52**, 97–106. https://doi.org/10.1007/s00603-018-1580-4 (2019). I. U.
34. Shouqing, L. U., Yongliang, Z. H. A. N. G., Zhanyou, S. A. & Shufang, S. I. Evaluation of the effect of adsorbed gas and free gas on mechanical properties of coal. *Environ. Earth Sci.* **78**, 1–15. https://doi.org/10.1007/s12665-019-8222-3 (2019).
35. Changbao, J. I. A. N. G., Yang, Y. A. N. G., Wenhui, W. E. I., Minke, D. U. & Tang, Y. U. A. N., A new stress-damage-flow coupling model and the damage characterization of raw coal under loading and unloading conditions. *Int. J. Rock. Mech. Min. Sci.* **138**, 104601. (2021). https://doi.org/10.1016/j.ijrmms.2020.104601
36. Xiuli, D. I. N. G., Xuanyan, F. A. N., Shuling, H., Peiyang, Y. U. & Jinxin, Z. H. A. U. A. N. G., N. G. Statistical damage model of mudstone considering hydration and swelling and its verification. *Chin. J. Rock Mech. Eng.* **42**(11), 2601–2612. (2023). https://doi.org/10.13722/j.cnki.jrme.2023.0155

Acknowledgements

This work was supported by National Major Scientific Instruments and Equipments Development Project of National Natural Science Foundation of China (52227804), Fund Project of Sinopec Petroleum Engineering Technology Research Institute (35800000-22-ZC0699-0004), The Open Research Fund of Jiangsu Key Laboratory of Construction Materials of Southeast University (No. 202508), Youth Program of National Natural Science Foundation of china (52404015).

Author contributions

Conceptualization, K.L. and H.Z.; Methodology, K.L. and X.L.; Formal Analysis, B.W. and B.Y.; Data Curation, K.L., Y.Z. and J.A.; Writing—Original Draft Preparation, K.L.; Writing—Review and Editing, H.Z. and Y.Z.; Visualization, B.Y. and X.L.; Supervision, K.L. and B.W.; All authors have read and agreed to the published version of the manuscript.

Declarations

Competing interests
The authors declare no competing interests.

Additional information
Correspondence and requests for materials should be addressed to H.Z.

Reprints and permissions information is available at www.nature.com/reprints.

Publisher's note Springer Nature remains neutral with regard to jurisdictional claims in published maps and institutional affiliations.